Journal of Ceramic Processing Research. Vol. 9, No. 6, pp. 672~677 (2008)

J O U R N A L O F
Ceramic Processing Research

Thermal properties of TiAlN and Ti-Al-O coated Inconel 617

Byeong Woo Lee[a], Do Wan Kim[a], Jong Won Choi[a], Kwang Hyun Bang[b], Gun Hwan Lee[c] and Hyun Cho[d,*]

[a]*Department of Materials Engineering, Korea Maritime University, Busan 606-791, Korea*
[b]*Division of Mechanical and Information Engineering, Korea Maritime University, Busan 606-791, Korea*
[c]*Advanced Thin Film Research Group, Korea Institute of Materials Science, Gyeongnam 641-831, Korea*
[d]*Department of Nanosystem and Nanoprocess Engineering, Pusan National University, Gyeongnam 627-706, Korea*

TiAlN and Ti-Al-O thin films (~3 mm) were deposited on Inconel 617 by an arc-discharge and a RF sputtering method, respectively. The effect of the coatings on the thermal stability and wear properties of the Inconel alloy after heat treatment up to 1000 °C has been studied. The uncoated Inconel 617, heat treated at 1000 °C, showed a poor wear resistance and an inferior thermal stability due to the formation of thick corrosion scales in addition to the distinctive hill-shape crusts, which are both composed of Cr_2O_3 on the alloy surface. Ti-Al-O coated samples heat treated at 1000 °C also showed a poor wear resistance due to the considerable amount of Cr_2O_3 scale formation. It has been found that the TiAlN coating layer decomposed at 1000 °C and was oxidized into a TiO_2-rich top-layer, followed by an Al_2O_3-rich layer between the top-layer and the alloy substrate. Since the dense protective oxide layers, which were oxidation products, prevented the formation of thick and brittle Cr_2O_3 scales (crusts) on the alloy surface, the TiAlN coated Inconel showed an enhanced thermal oxidation resistance and an increased wear resistance.

Key words: Ceramic coating, TiAlN and Ti-Al-O thin film, Inconel 617, Thermal property, Oxidation.

Introduction

Inconel 617, an advanced superalloy, has superior high temperature properties and finds application in thermal systems such as gas turbines and heat exchangers, where the alloy is subjected to the combined effects of corrosion, mechanical and thermal stresses [1-3]. In particular, this superalloy is one of the leading candidate materials for heat transport systems of the very high temperature reactor (VHTR), which is anticipated to operate at temperatures between 900 and 1000 °C [3, 4]. These are extremely challenging conditions for the operation of metallic components.

Inconel 617 is a nickel-base alloy, which mainly contains chromium, cobalt and molybdenum. A solid solution strengthening is provided by cobalt and molybdenum, and chromium provides the corrosion (oxidation) resistance at relatively high temperatures by forming a hard and dense diffusion barrier of an in-situ oxide film on the alloy surface [5, 6].

Considerable research has been carried out on the properties of Inconel alloys. It has been shown that Inconel alloys have relatively good mechanical properties over a relatively wide temperature range, but their wear and corrosion resistance are unsatisfactory at higher temperatures [7, 8]. The thin chromium oxide (Cr_2O_3) films formed in-situ on the alloy surface inhibit further oxidation due to the blocking of the inter-diffusion between the oxygen in the air and the chromium in the alloy at moderate temperatures. As the temperature increases further, however, the inter-diffusion will be accelerated, eventually resulting in the formation of thick, brittle and volatile Cr_2O_3 scales [5, 9]. Therefore the heat resistance of Inconel alloys at higher temperatures is limited by the instability of the Cr_2O_3 scales and this restricts the application range of Inconel alloys in an oxidizing atmosphere. Recently, surface modification of Inconel alloys using refractory ceramic coatings has received much attention since it can produce an increased high temperature stability against corrosion and wear [10-12].

In our previous research [13] on some titanium-based nitride films, including TiN, TiCN and TiAlN coatings for an Inconel alloy, it has been shown that the TiN and TiCN films start to decompose below 600 °C as reported elsewhere [14, 15] and turned to an oxide which was identified as TiO_2 (rutile), showing a poor thermal stability. As the oxidation progressed, surface defoliation over wide areas was observed for the TiN and TiCN coated samples. Also identical with the behavior of uncoated Inconel 617, thick Cr_2O_3 crusts especially along the grain boundary regions appeared at 1000 °C due to the film decomposition and defoliation. From a morphological, structural and tribological examination [13], it was found that, among the titanium-based nitride films, the TiAlN film showed superior high temperature properties in the temperature range (~1000 °C) for the Inconel 617 alloy.

In the present study, the thermal properties of Ti-Al-

*Corresponding author:
Tel : +82-55-350-5286
Fax: +82-55-350-5653
E-mail: hyuncho@pusan.ac.kr

based nitride (TiAlN) and oxide (Ti-Al-O) coated Inconel 617 have been investigated. The TiAlN and Ti-Al-O films have adjacent Ti/Al cation ratios and a comparative study of their morphological and micro-structural characteristics at temperatures up to 1000 °C has been conducted.

Experimental

1.6 mm thick plates of a commercial Inconel 617 alloy (Ni-22Cr-12.5Co-9Mo-1Al, wt%) manufactured by High Temperature Metals Inc. (USA) were used as substrates in the present study. Thin films of TiAlN (Ti/Al = 1.2) and Ti-Al-O (Ti/Al = 1.1) were coated on the Inconel 617 substrates. TiAlN films were deposited on the Inconel 617 by an arc-discharge technique. During the deposition process the substrate temperature and chamber pressure were fixed at 450 °C and 1×10^{-5} Torr (1.33×10^{3} μPa), respectively. Mixed oxide, Ti-Al-O, films were deposited by an RF (co-) sputtering process with the use of TiO_2 and Al_2O_3 double targets and the deposition was conducted at a substrate temperature of 750 °C, a chamber pressure of 2×10^{-2} Torr (2.66 Pa), and an Ar to O_2 ratio of 3. The film thickness was controlled to be ~3.0 μm for all specimens. The coated specimens were heat treated up to 1000 °C for 12-48 h in the air and analyzed.

The structural and compositional properties of the as-prepared and heat treated samples were characterized by X-ray diffraction (XRD, Cu-Kα), scanning electron microscopy (SEM), and energy dispersive X-ray spectroscopy (EDS). To evaluate the wear resistance of heat treated samples, wear loss was measured using a ball-on-disk type (ϕ6 mm ZrO_2 ball) wear testing system under the conditions of a test load of 5 kg and rotation speed 100 rpm. For the heat treated samples, the surface morphology and cross-section near surface compositions were also examined by SEM-EDS.

Results and Discussion

Microstructural evolution of the uncoated Inconel 617 at high temperatures

Fig. 1 presents polished and etched microstructures of the Inconel plates of (a) as-received and (b) heat treated at 1000 °C for 24 h, showing the mixed coarse and fine grains, no further grain growth in the heat-treated sample was found. This result indicates the stable nature of the Inconel 617 alloy (bulk or interior) at elevated temperatures. For both samples, coarse grains are around 100 μm in diameter, while the finer grains range from approximately 10 to 50 μm.

X-ray diffraction patterns of the Inconel 617 heat treated at various temperatures are shown in Fig. 2. The XRD results indicate that a noticeable amount of Cr-oxide (Cr_2O_3) appears at 950 °C and the content increases with temperature as well as heat treatment time. The Surface morphologies of the Inconel specimens heat treated at 1000 °C for 24 h are presented in Fig. 3. External oxide

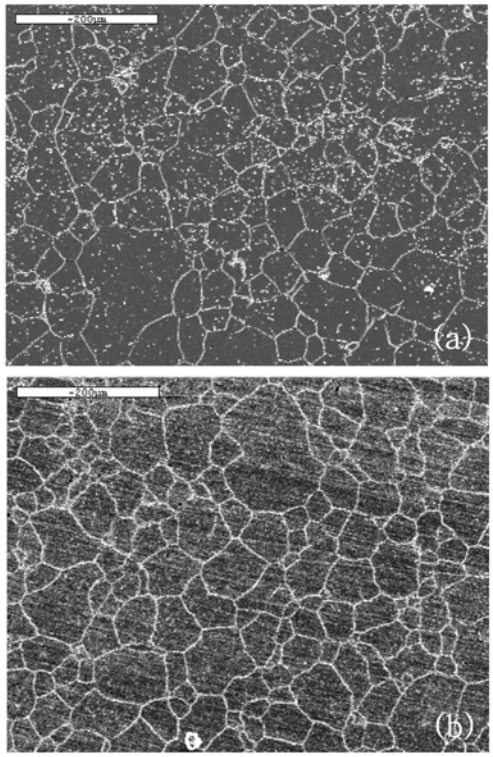

Fig. 1. SEM surface morphology of chemically etched Inconel 617: (a) untreated, and (b) heat treated at 1000 °C for 24 h (white bar: 200 μm).

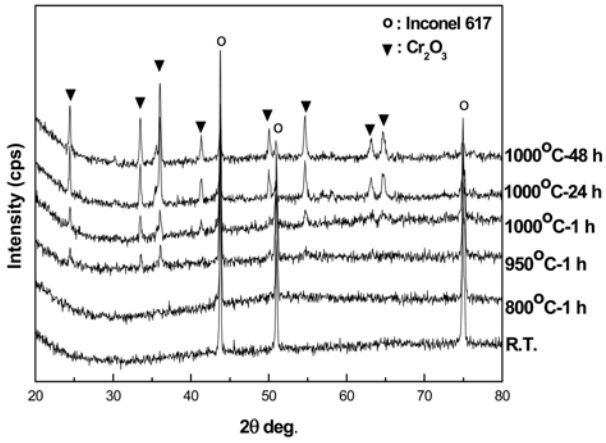

Fig. 2. X-ray diffraction patterns of Inconel 617 heat treated at different temperatures and times.

scales indexed as Cr_2O_3 are observed and the distinctive hill-shape crusts along with the grain boundaries are also observed. Fine 0.8-1.2 μm triangular crystallites are compactly formed on the hill (grain boundary) regions while somewhat bigger crystals, 2-3 μm, are formed on the base of the Inconel surface. It is assumed that the fine crystallite structure found on the hills was caused by the abundant nucleation due to the faster Cr diffusion to the metal surface along the grain boundaries, easily forming Cr_2O_3 crystallites with oxygen.

The surface morphology and cross-sectional micros-

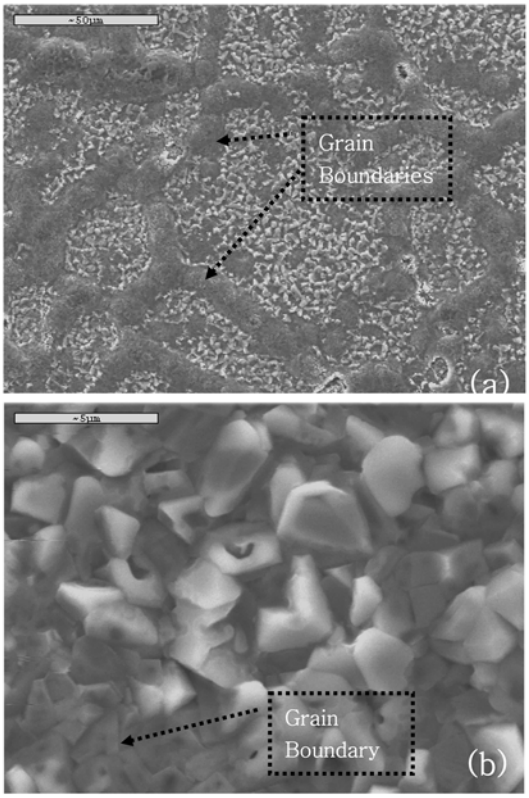

Fig. 3. SEM surface morphologies of Inconel 617 heat treated at 1000 °C for 24 h showing; (a) hill-shape Cr_2O_3 crusts along the grain boundaries (white bar: 50 μm), and (b) different crystallites sizes between the hill and the base (white bar: 5 μm).

tructures with compositional profiles determined by SEM-EDS for the samples heat treated at 1000 °C for 48 h are presented in Fig. 4. It was found that a distinct grain boundary structure still existed, while the increased heating time resulted in further crystallite growth (~2-3 μm) in the crusts at the grain boundaries. Furthermore, the overgrown hill-like structure has been weakened by the volume expansion resulting from the accelerated diffusion along the grain boundaries, in which a surface defoliation was often seen. External scales (crusts) composed of Cr and O are clearly observed in the cross-sectional SEM and EDS results, and the Ni-deficient surface structure indicates that the surface scales were formed by a reaction between oxygen in the air and internal Cr which had diffused out to the surface. It is assumed that the near-surface internal cavities (or pores) resulted from the Cr diffusion to the surface. In particular, the accelerated diffusion along the grain boundaries is considered to be the main reason for the sizable cavities relatively deep inside (> 10 μm) the metal as shown in Fig. 4(b).

Mechanical failure will be clearly influenced by the surface or near surface defects. It can therefore be stated that the large defect area having surface crusts with defoliation and the near surface cavities in the Inconel 617 as shown in Fig. 4 could make the material weaker and might induce an immature failure in use.

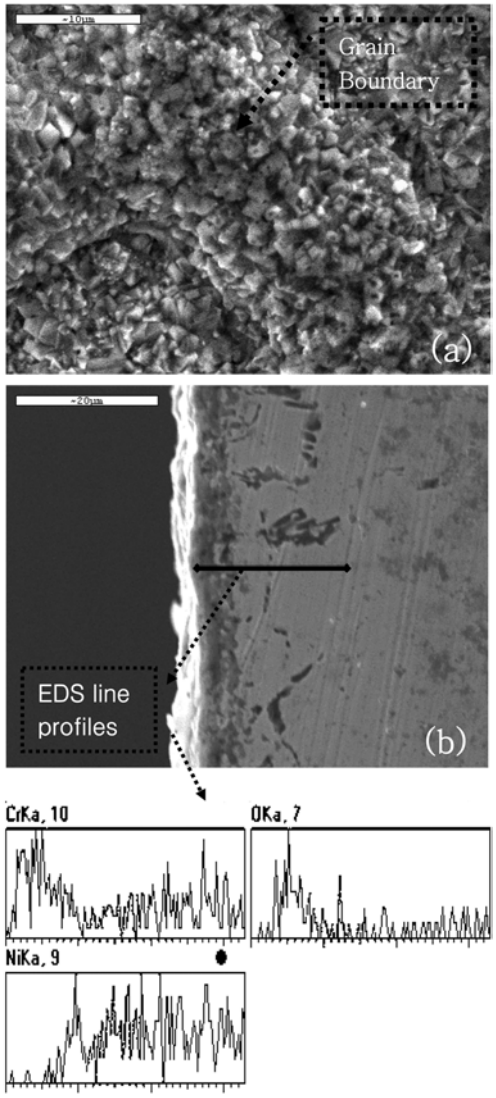

Fig. 4. SEM morphologies of Inconel 617 heat treated at 1000 °C for 48 h: (a) surface (white bar: 10 μm), and (b) cross-section (white bar: 20 μm, bottom: compositional depth profiles determined by EDS).

High-temperature thermal stability of the TiAlN and Ti-Al-O ceramic-coated Inconel 617

X-ray diffraction patterns of the TiAlN and Ti-Al-O coated Inconel 617 samples heat treated at different temperatures up to 1000 °C are presented in Fig. 5. For both the TiAlN and Ti-Al-O films heat treated at 1000 °C for 48 h, the identified phases are the same, namely TiO_2 and Cr_2O_3. In the case of the TiAlN-coated Inconel, the nitride films are decomposed at temperatures above 800 °C In contrast to the results for the uncoated and Ti-Al-O coated Inconel, the in-situ Cr_2O_3 formation for the TiAlN-coated samples was considerably suppressed towards higher heat treatment temperatures and heating times. At the decomposition (oxidation), only rutile peaks from titanium dioxide could be identified and there was no indication of crystalline Al_2O_3 peaks in the XRD result. The absence of Al_2O_3 peaks by forming an amorphous Al-oxide in oxidized Ti-Al-N films is identical with the

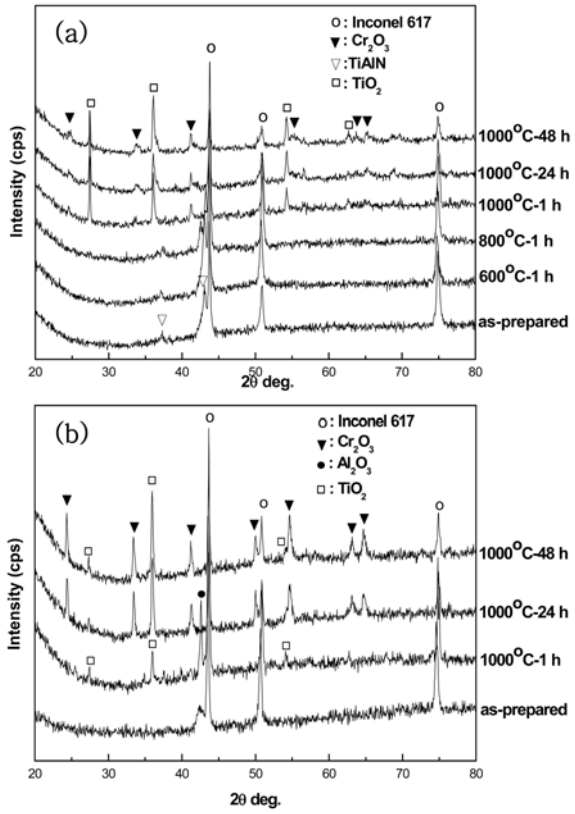

Fig. 5. X-ray diffraction patterns of (a) TiAlN coated, and (b) Ti-Al-O coated Inconel 617 heat treated at different temperatures and times.

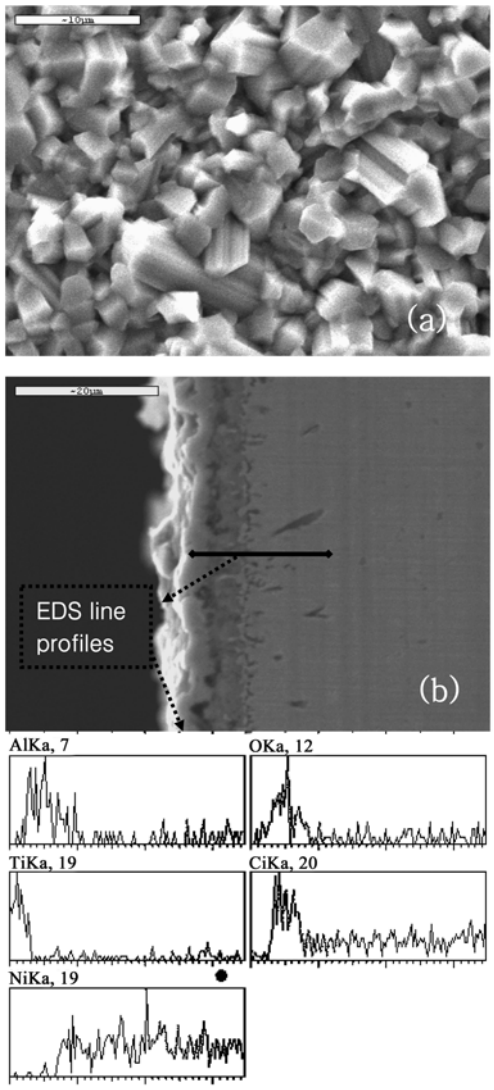

Fig. 6. SEM morphologies of TiAlN coated Inconel 617 heat treated at 1000 °C for 48 h: (a) surface (white bar: 10 μm) and (b) cross-section (white bar: 20 μm, bottom: compositional depth profiles determined by EDS).

results previously reported [15-17].

The surface and cross-sectional SEM micrographs and associated EDS compositional profiles of a TiAlN coated Inconel 617 sample, heat treated at 1000 °C for 48 h, are shown in Fig. 6. A dense crystallized coating layer, with no defoliation and no hill-like structures was found (Fig. 6(a)). The cross-sectional depth profile, compared to the case of the uncoated Inconel, clearly shows a smaller affected area having a reduced number and size of pores or cavities. The EDS compositional analysis reveals that the outermost surface is mainly composed of Ti and beneath the top-layer Al and Cr coexist. In the light of the XRD results combined with the cross-sectional EDS analysis, the top-layer is a TiO_2 (rutile) rich phase and in the sub-layer, between the top-layer and the Ni-based metal substrate, Cr_2O_3 and an amorphous Al-oxide phase coexist. The reactive Al diffuses towards the metal forming a dense sub-layer, which eventually leaves a TiO_2-rich top-layer. Once the dense surface TiO_2 layer and Al containing sub-layer form, the inwards diffusion of oxygen through the dense layers is hindered to a considerable extent, and then further chromium oxide formation is suppressed. Therefore, the hill-like structures caused by the inhomogeneous grain boundary diffusion are also inhibited.

X-ray diffraction patterns of the Ti-Al-O coated Inconel 617 show that only Al_2O_3 peaks are identified in the as-prepared sample (Fig. 5(b)). As the heat treatment temperature and time increase, the Al_2O_3 peaks disappear and the TiO_2 (rutile) peaks are observed with considerably intense Cr_2O_3 peaks. From the XRD results combined with the SEM-EDS analysis (Fig. 7) of the Ti-Al-O coated Inconel heat treated at 1000 °C for 48 h, Al diffused into the deep inside from the surface and Cr which had diffused out from the alloy resulted in the distinctive composition lines including a Cr_2O_3-rich layer (darker line in Fig. 7) sandwiched in between TiO_2-rich layers. In the case of the Ti-Al-O coated Inconel, the Al diffused into the metal in deeper inside showing Al and Ni coexistence. Also identical with the TiAlN coating, Al_2O_3 peaks were not found in the Ti-Al-O coated Inconel 617 heat treated at elevated temperatures (~1000 °C), resulting from the formation of an Al amorphous compound formation in deep inside the alloy. It is suggested that the high reactivity of the Al component in the Ti-Al-O coating leads to the enhanced inward diffusion combining

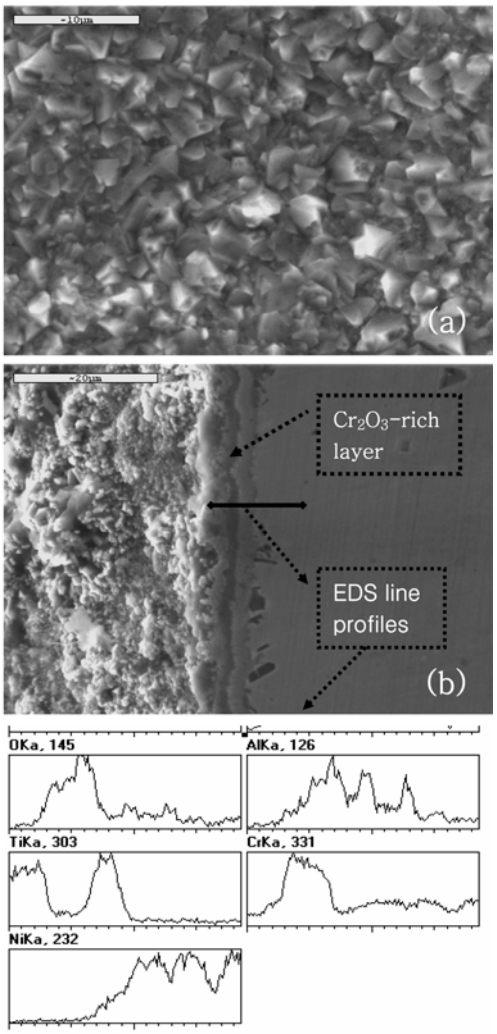

Fig. 7. SEM morphologies of Ti-Al-O coated Inconel 617 heat treated at 1000 ºC for 48 h: (a) surface (white bar: 10 μm) and (b) cross-section (white bar: 20 μm, bottom: compositional depth profiles determined by EDS).

with the extensive Cr outward diffusion resulting in the formation of considerable amount of Cr_2O_3 as shown in the XRD result (Fig. 5(b)). The mechanism behind these phenomena is not yet fully elucidated. Although there are relatively large amounts of Cr_2O_3 formation in the Ti-Al-O coated alloy, no hill-like structures were found (Fig. 7(a)).

Fig. 8 shows wear test results for the bare (uncoated), TiAlN, and Ti-Al-O coated Inconel 617 samples after heat treatment at 1000 ºC for 24 h. There is a little improvement in the wear resistance of the Ti-Al-O coated Inconel 617 compared to the uncoated Inconel 617 due to the relatively large amount of Cr_2O_3 formation as described above. Far from a protective film, the Cr_2O_3 layer just acts as a brittle crust. The TiAlN-coated Inconel 617 samples represent the best performance, most likely due to the formation of protecting oxide layers with a reduced amount of Cr_2O_3 formation, which is consistent with the XRD and microstructural analysis presented above.

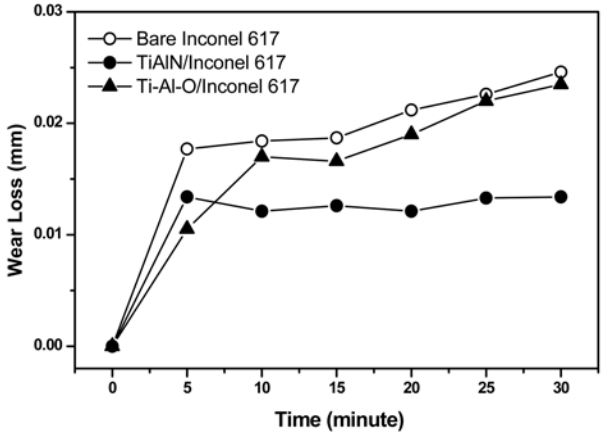

Fig. 8. Wear loss of bare (uncoated), TiAlN, and Ti-Al-O coated Inconel 617 heat treated at 1000 ºC for 24 h.

Conclusions

The microstructural properties of two different ceramic coatings (TiAlN and Ti-Al-O) and their effects on the wear resistance and thermal oxidation behavior of Inconel 617 alloy up to 1000 ºC have been studied. Uncoated Inconel 617 showed a poor thermal stability at elevated temperatures (~1000 ºC), forming a thick corrosion scale (Cr_2O_3) as well as distinctive hill-shape crusts along the grain boundaries. Compared to the bare Inconel alloy, the Ti-Al-O-coated samples heat treated at 1000 ºC showed only a negligible improvement in wear resistance because of the formation of a considerable amount of Cr_2O_3. The TiAlN coated Inconel showed an enhanced thermal stability. At elevated temperatures, the TiAlN coating turned into dense protective oxide layers preventing the formation of thick and brittle Cr_2O_3 scales on the alloy surface. The increased wear resistance for the TiAlN coated Inconel could also be attributed to the suppressed Cr_2O_3 formation. Therefore TiAlN is thought to be a promising coating layer for Inconel 617, which might be used in very high temperature applications above 900 ºC.

Acknowledgment

This research was performed under the program of Basic Atomic Energy Research Institute (BAERI), which is a part of the Nuclear R&D Programs funded by the Ministry of Science & Technology (MOST) of Korea.

References

1. P.R. Sahn and M.O. Speidal, High Temperature Materials in Gas Turbines, Elsevior, New York (1974).
2. M.K. Ali, M.S.J. Hashmi, and B.S. Yilbas, J. Mater. Process. Technol. 118 (2001) 45-49.
3. T. C. Totemeier and H. Tian, Mater. Sci., Eng. (2007) 81-87.
4. Next Generation Nuclear Plant Materials Research and Development Program Plan, INEEL/EXT-04-02347 (2004).
5. M.J. Donachie and S.J. Donachie, Supperalloys, ASM

International, OH (2002).
6. J.R. Davis, Heat-Resistant Materials, ASM International, OH (1997).
7. L. Jian, C.Y. Yuh, and M. Farooque, Corrs. Sci. 42 (2000) 1573-1585.
8. B.S. Yilbas, M. Khaled, and M.A. Gondal, Optics and Lasers in Eng. 36 (2001) 269-276.
9. M. Tacikowski, J. Stoma, M. Wozniak, and T. Wierzchon, Intermetallics 14 (2006) 123-129.
10. M. Shindo and H. Nakajima, ISIJ Int. 29 (1989) 793-795.
11. T. Takeda, K. Kunitomi, M. Ohkubo, and T. Saito, Nucl. Eng. Des. 185 (1998) 229-240.
12. K.A. Gruss and R.F. Davis, Surf. Coat. Technol. 114 (1999) 156-168.
13. H. Cho, D.M. Lee, J.H. Lee, H.S. Lee, K.H. Bang, and B.W. Lee, J. Ceram. Process. Res. 8 (2007) 453-457.
14. J.H. Hsieh, A.L.K. Tan, and X.T. Zeng, Surf. Coat. Technol. 201 (2006) 4094-4098.
15. A. Mitsuo, S. Uchida, N. Nihira, and M. Iwaki, Surf. Coat. Technol. 103-104 (1998) 98-103.
16. C.T. Huang and J.G. Duh, Surf. Coat. Technol. 81 (1996) 164-171.
17. A. von Richthofen, R. Cremer, M. Witthaut, R. Domnick, and D. Neuschütz, Thin Solid Films 312 (1998) 190-194.